Modeling of scattering and depolarizing electro-optic devices. I. Characterization of lanthanum-modified lead zirconate titanate

Paul E. Shames, Pang Chen Sun, and Yeshaiahu Fainman

We describe a new method of modeling electro-optic (EO) devices, such as lanthanum-modified lead zirconate titanate polarization modulators, that resolves two deficiencies of current methods: (i) the inclusion of depolarization effects resulting from scattering and (ii) saturation of the EO response at strong electric-field strengths. Our approach to modeling depolarization is based on describing the transmitted optical field by superposition of a deterministic polarized wave and a scattered, randomly polarized, stochastic wave. Corresponding Jones matrices are used to derive a Mueller matrix to describe the wave propagation in scattering and depolarizing EO media accurately. A few simple optical measurements can be used to find the nonlinear behavior of the EO phase function, which is shown to describe accurately the material's EO behavior for weak and strong applied electric fields. © 1998 Optical Society of America

OCIS codes: 160.2100, 190.5890, 080.2730, 190.3270, 260.2130.

1. Introduction

Polycrystalline lanthanum-modified lead zirconate titanate (PLZT) is an electro-optic (EO) material that has many advantages over single-crystal EO materials, including ease of manufacturing, low operating voltages, and reduced long-range strain effects.[1] PLZT-based devices with compositions of 8.8–9.5/65/35 are used in a variety of optoelectronic applications including high-speed scanning,[2] dynamic lenses,[3] optical switches,[4] and shutters and eye-protection devices.[5]

Bulk PLZT can be highly scattering, which has constrained the geometry of many devices to the use of thin wafers with interdigital surface-electrode designs. These design geometries can require the application of very strong electric fields. For example, consider a programmable phased-array device that uses PLZT 9.0/65/35 with surface electrodes separated by 40 μm. To achieve an average phase shift of $\phi \approx \pi$ for light passing through such a device requires applying field strengths greater than 1.5×10^6 V/m throughout the gap region. At these field strengths, we have found that even thin wafers of PLZT become highly scattering.[6] This scattering can significantly reduce the optical signal strength, create off-axis noise, and depolarize the transmitted light.[7] Therefore design geometries that reduce the operating electric-field strength and the associated scattering and depolarizing effects are critical for PLZT-based devices.

Computer-aided design and modeling, or CAD–CAM, can be a very useful tool in the development of EO device geometries for improved performance. Traditionally,[8–13] these EO devices are modeled by use of a simple Jones calculus[14] model that cannot account for the effects of depolarization. Additionally, PLZT 8.8–9.5/65/35 device phase modulation is usually modeled by a classical Kerr quadratic EO effect[1,3] or a combination of linear and quadratic effects[5,15,16] (i.e., second-order effects). These models fail to describe accurately both the weak and the strong electric-field-induced EO response.

To achieve accurate computer simulation, particularly for devices that experience strong electric fields, it is necessary to take into account scattering and the resultant depolarization effects, and a higher than second-order EO phase function must be used. To derive a model that can account for depolarization,

The authors are with the Department of Electrical and Computer Engineering, University of California, San Diego, 9500 Gilman Drive, La Jolla, California 92093-0407.

Received 13 October 1997; revised manuscript received 2 March 1998.

0003-6935/98/173717-09$15.00/0

we describe the optical field transmitted through a scattering EO medium by superposition of a deterministic polarized wave and a scattered, randomly polarized, stochastic wave. The vector properties of such optical fields are then described by the corresponding superposition of a deterministic and a stochastic Jones matrix. The resulting Jones matrices are used to derive a Mueller matrix to describe accurately the wave propagation in a scattering EO medium. A few simple optical measurements can be used to characterize the material for the Mueller matrix coefficients. In addition, using the same set of measurements we solve for an EO function that accurately describes the change in relative phase between two orthogonal polarization components parallel and perpendicular to an applied electric field. Applying this method to PLZT 8.8–9.5/65/35, we find that, in contrast to the traditional quadratic EO model, the derived EO phase response is best fitted with a fifth-order polynomial function. This higher-order phase function accounts for the experimentally observed EO response that is due to weak as well as strong applied electric fields.

In this manuscript (part 1 of two papers) we derive our simplified Mueller matrix model and discuss its application to characterizing PLZT; the application of this technique to device modeling is reported in the second paper, in this issue (see pp. 3726–3734). We show how a few simple optical transmission measurements account fully for the electric-field-induced response of the material while allowing for the solution of an accurate EO function. In Section 2 we begin our discussion with a review of the various electric-field-induced effects that are included in our model. In Section 3 we use Stokes vectors and Mueller matrices to describe optical beam transmission through depolarizing systems. We then present in Section 4 our experimental characterization of a sample of PLZT material and compare the results to our new model. Finally, in Section 5 we give a summary and conclusions.

2. Electric-Field-Induced Effects

PLZT is a ferroelectric ceramic material composed of crystallites, varying 1–10 μm in grain size,[17] whose material phase (and electrical characteristics) are sensitive to changes in material composition, temperature, and applied electric field. In the absence of an applied electric field the PLZT is optically isotropic, whereas an applied electric field induces refractive-index anisotropy. This leads to an optical phase difference ϕ for two orthogonally polarized light components passing through the material (e.g., parallel to and perpendicular to the direction of the applied field). Figure 1(a) shows a typical experimental setup for the measurement of transmitted light intensity through a PLZT sample by use of crossed polarizers set at 45° relative to the applied-field direction. Traditionally, the relative phase change (i.e., the EO response of the material) is assumed to be quadratic, that is, $\phi \propto E^2$, where E is the magnitude of the applied electric field. The transmission intensity I of light through such a system is usually modeled by use of Jones calculus by the relation

$$I = \frac{1}{2}\sin^2\left(\frac{\phi}{2}\right), \tag{1}$$

where the intensity reaches maxima and minima [see Fig. 1(b)] when $\phi = n\pi$ (where n is an integer). However, a typical experimental result of intensity measurements as shown in Fig. 1(b) illustrates how a real device's EO response departs from this simple analytic model. At low field strength there is almost no EO response, and the quadratic phase model needs to be shifted [i.e., $\phi \propto (E - E_0)^2$] to take this weak response into account. At high field strength we can see that the EO effect diminishes (i.e., the period increases) compared to the quadratic approx-

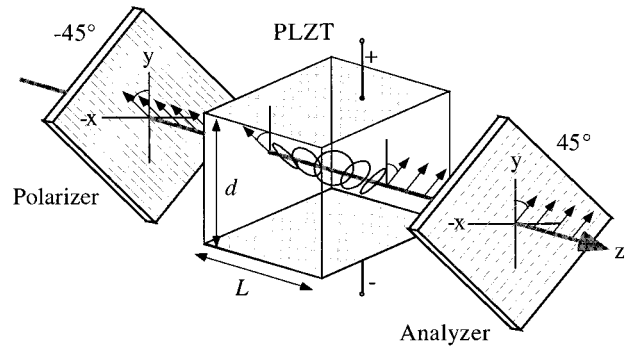

(a)

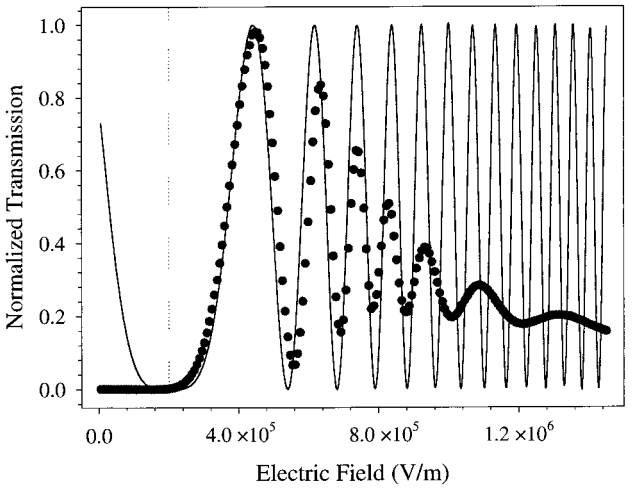

(b)

Fig. 1. (a) PLZT sample with transverse electrodes oriented to generate an electric field along the y axis. A crossed polarizer–analyzer pair is oriented at 45° and −45°, respectively, to the y axis. Linear polarized light is rotated 90° if the induced birefringence results in a phase difference of $\phi = \pi$. (b) Experimental measurement results (filled circles) of the transmission intensity of light passing through the system as a function of the electric-field strength (for a PLZT sample of $L = 388$ μm). The solid curve shows the simulated performance by use of Eq. (1) and a best-fit quadratic EO model. To account for the weak EO response at low electric fields, a constant field of $E_0 = 2 \times 10^5$ V/m, opposite to the applied field direction, is included in the model.

imation. We can conclude that the quadratic EO model is accurate for only a limited range of the applied electric-field strength. The technique to generate a more accurate EO phase function, which can account for the weak and the strong electric-field response of this material, is discussed in Section 4.

In Fig. 1(b) we can also see that the transmitted optical intensity, as well as the contrast ratio, decrease as functions of the applied electric-field strength. The decrease in the measured intensity is due to scattering, which in PLZT has been found to be a function of material composition,[1] grain size,[17] and strength of the applied electric field.[7] The field-induced scattering can be related to index changes at grain and domain boundaries and with small strain-relieving domain formations.[18] For the majority of spatial light modulator devices, scattering introduces unwanted signal attenuation. Furthermore, the scattered light is depolarized,[7] and the portion that remains within the solid angle of the system's exit pupil creates noise in the detected signal. As the applied electric field is increased, the intensity of the detected depolarized light also increases, which can be seen as increases in the minima intensities for the transmission curve shown in Fig. 1(b). At high field strength the light is completely unpolarized, and we can no longer detect any change in relative phase.

3. Mueller Matrix Model for PLZT-Based Devices

Jones 1×2 vectors and 2×2 matrices are convenient tools for describing polarized light propagating through nondepolarizing optical devices and systems. However, to model depolarizing optical devices such as PLZT-based modulators, one must use a higher-order matrix representation.[19] In our case we use Stokes vectors[20] and Mueller matrices[21,22] (1×4 and 4×4, respectively). Consider a normally incident quasi-monochromatic optical beam with a mean frequency $\bar{\nu}$. Using a right-handed Cartesian coordinate system, as shown in Fig. 1(a), with the direction of propagation along the z axis, we obtain the two orthogonal complex electric-field components by

$$E_x(t) = E_1(t)\exp(i[\alpha_1(t) - 2\pi\bar{\nu}t]),$$
$$E_y(t) = E_2(t)\exp(i[\alpha_2(t) - 2\pi\bar{\nu}t]), \tag{2}$$

where the absolute phase $\{\alpha_1(t), \alpha_2(t)\}$ and amplitudes $\{E_1(t), E_2(t)\}$ of each component are real functions of time. The Stokes parameters, which are used to describe the polarization state of the light, are given in vector form by

$$\mathbf{S} \equiv \begin{bmatrix} S_0 \\ S_1 \\ S_2 \\ S_3 \end{bmatrix} \equiv \begin{bmatrix} \langle E_1^2 \rangle + \langle E_2^2 \rangle \\ \langle E_1^2 \rangle - \langle E_2^2 \rangle \\ 2\langle E_1 E_2 \cos\delta(t) \rangle \\ 2\langle E_1 E_2 \sin\delta(t) \rangle \end{bmatrix}, \tag{3}$$

where $\delta(t) = \alpha_1(t) - \alpha_2(t)$ is the relative phase difference between the two orthogonal components.

Transformation of the Stokes vector by a nonimaging[21] device, such as a polarizer or a phase retarder, is described by a 4×4 Mueller matrix $\mathbf{M}$. An optical system comprising a cascade of N such devices is represented by the product of their respective Mueller matrices:

$$\mathbf{M}_{\text{system}} = \mathbf{M}_N \mathbf{M}_{N-1} \ldots \mathbf{M}_n \ldots \mathbf{M}_1, \tag{4}$$

where $\mathbf{M}_{\text{system}}$ is the Mueller matrix representation of the entire optical system and $\mathbf{M}_n$ is the matrix of the nth device of the system. The transformation of the Stokes vector by an optical system is given by

$$\mathbf{S}_{\text{out}} = \mathbf{M}_{\text{system}} \mathbf{S}_{\text{in}}. \tag{5}$$

Given a known Jones matrix $\mathbf{J}$ (see Appendix A, Subsection 1), describing a nondepolarizing optical element, the corresponding Mueller matrix is given[21] by the transformation

$$\mathbf{M} = \mathbf{T}(\mathbf{J} \otimes \mathbf{J}^*)\mathbf{T}^{-1}, \tag{6}$$

where the symbol $\otimes$ denotes the Kronecker product[23] (see Appendix A, Subsection 2), the asterisk denotes the complex conjugate, and $\mathbf{T}$ is the 4×4 linear transformation between the Stokes parameters and the coherency matrix parameters[24] (see Appendix A, Subsection 3). As an example, for an ideal nonscattering and nondepolarizing EO device the Jones matrix is the same as a linear phase retarder and is given[10] by

$$\mathbf{J}(\phi) = \begin{bmatrix} \exp\left(i\frac{\phi}{2}\right) & 0 \\ 0 & \exp\left(-i\frac{\phi}{2}\right) \end{bmatrix}, \tag{7}$$

where ϕ is the relative phase difference for the x- and y-polarization components of the light. Substituting Eqs. (7), (A5), and (A9) into Eq. (6), we find the corresponding Mueller matrix[25]:

$$\mathbf{M}_{\text{PLZT}_{\text{ideal}}}(\phi) = \begin{bmatrix} 1 & 0 & 0 & 0 \\ 0 & 1 & 0 & 0 \\ 0 & 0 & \cos(\phi) & -\sin(\phi) \\ 0 & 0 & \sin(\phi) & \cos(\phi) \end{bmatrix}. \tag{8}$$

However, for a real PLZT device that has random scattering and depolarization one must use an ensemble average of Jones matrices.[24] To create such an ensemble, we distinguish in our model between the spatial frequency of the light incident upon and the spatial frequency of the light exiting the PLZT device, i.e., because of scattering we expect that the light exiting the device will have additional spatial-frequency components. For example, in our experiment we use a plane wave, i.e., with a single spatial frequency, which we define as the dc spatial-frequency optical field parallel to the optical axis, incident upon our PLZT device, whereas the exiting light is scattered and consists of a wide band of spatial-frequency components. Under the assumption that the scattering field from every point can be modeled as a zero-mean Gaussian random process,[26] we can separate the optical field transmitted through the PLZT device into two components: a nonscat-

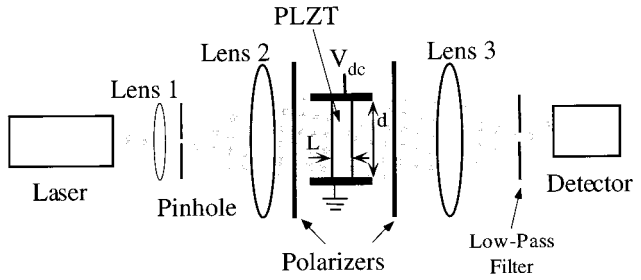

Fig. 2. Experimental setup for the characterization and modeling of PLZT samples. The PLZT sample is fully illuminated to avoid localized photorefractive effects. The low-pass filter was only used for experimental measurements for which the scattered fields needed to be filtered out.

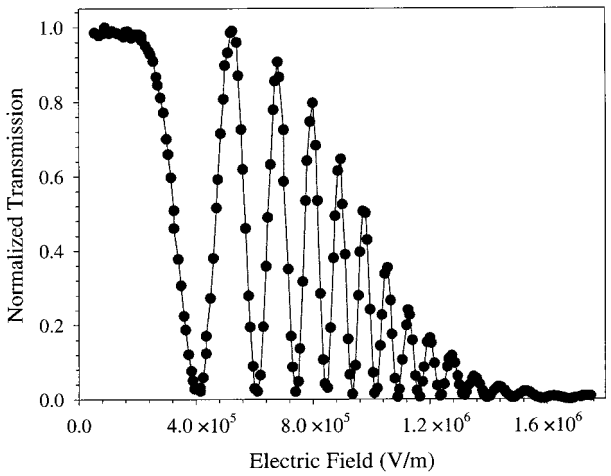

Fig. 3. Using a low-pass filter (see Fig. 2), we remove the scattered light from the detected signal. The remaining dc component contains no optical bias, allowing us to conclude that the dc light is polarized. In this measurement we used parallel polarizers, which resulted in a maximum intensity at zero voltage. The PLZT sample used was 1 mm thick, which accounts for the increase in phase variation compared with Fig. 1(b).

tered dc field and the scattered field. By using a low-pass filter (see Fig. 2) in the spatial Fourier transform plane of the output lens, we are able to filter the scattered light out from the output signal. Experimental measurements of such a system show (see Fig. 3) that the dc field is polarized and has a negligibly small scattered or depolarized component, which justifies the use of our superposition model. Therefore we conclude that only the scattering field contributes to the depolarization, which can be described by an ensemble of randomly polarized fields.[24]

We describe a typical PLZT-device Jones matrix by a superposition of a deterministic matrix, which accounts for the DC field, and an ensemble of nondeterministic matrices, which represents the scattered unpolarized field, [indicated by the superscript (e)], given by

$$\mathbf{J}^{(e)} = \begin{bmatrix} a\exp\left(i\frac{\phi}{2}\right) & 0 \\ 0 & b\exp\left(-i\frac{\phi}{2}\right) \end{bmatrix} + \begin{bmatrix} u_1 & u_3 \\ u_4 & u_2 \end{bmatrix}^{(e)} = \begin{bmatrix} a\exp\left(i\frac{\phi}{2}\right) + u_1^{(e)} & u_3^{(e)} \\ u_4^{(e)} & b\exp\left(-i\frac{\phi}{2}\right) + u_2^{(e)} \end{bmatrix}, \quad (9)$$

where a and b are the real transmittance amplitudes of the nonscattered light, ϕ is the relative phase difference for the two orthogonal polarization components, and $u_i^{(e)}$ are the complex transmittance amplitudes that account for the randomly polarized light. The coefficients u_1 and u_2 represent the amplitudes of the depolarized x and y light components, respectively, and u_3 and u_4 are the coupled or cross-depolarization amplitudes.

We assume that $u_i^{(e)}$ are independent random variables with a zero mean, $\langle u_i\rangle_e = 0$, and under the ensemble over a large detection area (e.g., a power meter much larger than the coherence area of the scattered light) the unpolarized components can be considered uncorrelated with each other as well as with the deterministic polarized components, i.e.,

$$\langle u_i u_k{}^*\rangle_e = \begin{cases} 0 & \text{if } i \neq k \\ U_i & \text{if } i = k \end{cases}, \quad (10)$$

$$\left\langle u_i \exp\left(\pm j\frac{\phi}{2}\right)\right\rangle_e = 0, \quad (11)$$

where $\langle \ldots \rangle_e$ is shorthand notation for the average over the ensemble and $U_i \equiv |u_i|^2$. The transformation for the ensemble average of Jones matrices into a Mueller matrix then takes the form[24] of

$$\mathbf{M} = \mathbf{T}\langle \mathbf{J}^{(e)} \otimes \mathbf{J}^{(e)*}\rangle_e \mathbf{T}^{-1}. \quad (12)$$

Using Eqs. (10) and (11) allows the resultant Mueller matrix to be written as

$$\mathbf{M}_{\mathrm{PLZT}} = \begin{bmatrix} \frac{1}{2}(A+B+U_1+U_2+U_3+U_4) & \frac{1}{2}(A-B+U_1-U_2-U_3+U_4) & 0 & 0 \\ \frac{1}{2}(A-B+U_1-U_2+U_3-U_4) & \frac{1}{2}(A+B+U_1+U_2-U_3-U_4) & 0 & 0 \\ 0 & 0 & \sqrt{AB}\cos(\phi) & -\sqrt{AB}\sin(\phi) \\ 0 & 0 & \sqrt{AB}\sin(\phi) & \sqrt{AB}\cos(\phi) \end{bmatrix}, \quad (13)$$

where we have used the definitions $A \equiv a^2$ and $B \equiv b^2$, which represent the intensity of the nonscattered light for the two orthogonally polarized light components, and U_i are the intensities of the depolarization components as defined in Eq. (10). As discussed in Section 2, the nonscattered and depolarized intensities as well as the change in phase are all functions of applied electric field. However, for simplicity we use the abbreviated forms

$$A(E) = A, \qquad B(E) = B,$$
$$U_i(E) = U_i, \qquad \phi(E) = \phi, \tag{14}$$

where E is the magnitude of the applied electric field. A similar matrix[27] has been obtained for a reflector with incoherent scattering (i.e., depolarization). However, in that case the cross-scattering is assumed to be negligible (i.e., $U_3 = U_4 = 0$). Applying such a matrix in our system, we find that the resultant Stokes parameters do not coincide with our experimental data. Therefore we need to include the cross-depolarization terms in our derivation.

Having derived an appropriate Mueller matrix for a PLZT device, we need to calculate the transformation of our complete experimental optical system and determine what set of intensity measurements will allow us to solve for the unknown coefficients. Our measurement apparatus uses normally incident coherent monochromatic light, polarized at 45° relative to the x axis [see Fig. 1(a)]. For our experiments the incident Stokes vector is determined by use of Eq. (3) with the maximum intensity normalized to 1 and under the assumption that $E_1(t) = E_2(t)$ and $\delta(t)$ is constant, which result in

$$\mathbf{S}_{\text{in}} = \begin{bmatrix} 1 \\ 0 \\ 1 \\ 0 \end{bmatrix}. \tag{15}$$

The light passes through a cascade of optical components made up of a polarizer, a PLZT device, and a second polarizer. The Mueller matrix for an ideal polarizer[25] is

$$\mathbf{M}_{\text{Pol}}(\theta) = \frac{1}{2}\begin{bmatrix} 1 & \cos(2\theta) & \sin(2\theta) & 0 \\ \cos(2\theta) & \cos^2(2\theta) & \cos(2\theta)\sin(2\theta) & 0 \\ \sin(2\theta) & \cos(2\theta)\sin(2\theta) & \sin^2(2\theta) & 0 \\ 0 & 0 & 0 & 0 \end{bmatrix}, \tag{16}$$

where θ is the angle between the polarizer axis and the x axis. The output Stokes vector is obtained with the transformation given by Eq. (5) applied to our system, yielding

$$\mathbf{S}_{\text{out}} = \mathbf{M}_{\text{Pol}}(\theta_a)\mathbf{M}_{\text{PLZT}}\mathbf{M}_{\text{Pol}}(\theta_p)\mathbf{S}_{\text{in}}, \tag{17}$$

where θ_p is the angle of the first polarizer and θ_a is the angle of the second polarizer (usually referred to as the polarizer and the analyzer, respectively), with $\mathbf{M}_{\text{PLZT}}$ from Eq. (13).

From the Mueller matrix [Eq. (13)] for the PLZT device we have seven unknown coefficients: A, B, U_1, U_2, U_3, U_4, and ϕ, which represent the intensities of the nonscattered polarized light, the depolarized light, and the change in the relative phase between the orthogonally polarized components. Our objective is to find equations of measured intensity that allow us to solve for the seven unknowns that will characterize the PLZT sample as functions of E, the applied electric-field strength. The first component of the output Stokes vector represents the measured optical intensity. It can be described as a function of the two polarizer angles: $S_{0_{\text{out}}} = I_{\theta_a,\theta_p}$. Using five convenient pairs of polarizer–analyzer angles in Eq. (17), we solve for $S_{0_{\text{out}}}$ and find

$$I_{45°,45°} = \frac{1}{4}\{A + B + U_1 + U_2 + U_3 + U_4 + 2\sqrt{AB}\cos(\phi)\}, \tag{18}$$

$$I_{0°,0°} = \frac{1}{2}(A + U_1), \tag{19}$$

$$I_{90°,90°} = \frac{1}{2}(B + U_2), \tag{20}$$

$$I_{0°,90°} = \frac{1}{2}U_3, \tag{21}$$

$$I_{90°,0°} = \frac{1}{2}U_4, \tag{22}$$

where we have normalized the incident light intensity. Equations (19) and (20) each contain one polarized component and one depolarized component. By subtracting the depolarized component by use of the low-pass filtering technique described above, we can reduce these equations to

$$I_{0°,0°-\text{Filter}} = \frac{1}{2}A, \tag{23}$$

$$I_{90°,90°-\text{Filter}} = \frac{1}{2}B. \tag{24}$$

Here we normalize the measurements with respect to the intensity at zero applied voltage after the low-pass filter. Including Eqs. (23) and (24), we have derived seven equations [Eqs. (18)–(24), representing seven experimental measurements] required to characterize the PLZT sample fully, i.e., the seven coefficients that represent the intensity of the polarized components (A and B), the depolarized components (U_1, U_2, U_3, and U_4), and the change in relative phase (ϕ).

If we wish to reduce the number of required measurements, we can assume that the scattering is isotropic. This results in the amplitudes and intensities of the polarized components being identi-

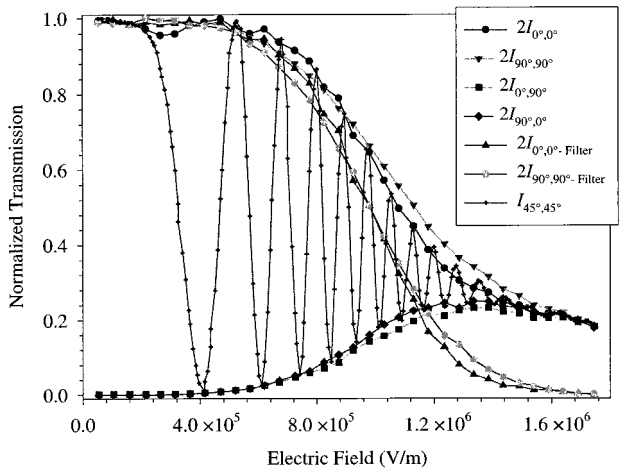

Fig. 4. Seven optical intensity measurements normalized to illustrate the envelope functionality of the vertical and horizontal components to the $I_{45°,45°}$ data.

cal, i.e., $A = B$, and the various depolarization intensity coefficients U_i would also be equivalent, i.e.,

$$U = U_i, \qquad \{i = 1, 2, 3, 4\}. \tag{25}$$

Equation (13) reduces to

$$\mathbf{M}_{\mathrm{PLZT}} = \begin{bmatrix} A + 2U & 0 & 0 & 0 \\ 0 & A & 0 & 0 \\ 0 & 0 & A\cos(\phi) & -A\sin(\phi) \\ 0 & 0 & A\sin(\phi) & A\cos(\phi) \end{bmatrix}. \tag{26}$$

We now require only three equations to solve for the coefficients, for example:

$$I_{45°,45°} = \frac{1}{2}\{A + 2U + A\cos(\phi)\}, \tag{27}$$

$$I_{0°,0°} = I_{90°,90°} = \frac{1}{2}(A + U), \tag{28}$$

$$I_{0°,90°} = I_{90°,0°} = \frac{1}{2}U. \tag{29}$$

In Section 4 we describe experimental measurement data (Fig. 4) showing that, for the PLZT samples used, the isotropic approximation is acceptable.

Finally, the Mueller matrix of Eq. (26) can be decomposed into deterministic and nondeterministic parts:

$$\mathbf{M}_{\mathrm{PLZT}} = \begin{bmatrix} A & 0 & 0 & 0 \\ 0 & A & 0 & 0 \\ 0 & 0 & A\cos(\phi) & -A\sin(\phi) \\ 0 & 0 & A\sin(\phi) & A\cos(\phi) \end{bmatrix} + \begin{bmatrix} 2U & 0 & 0 & 0 \\ 0 & 0 & 0 & 0 \\ 0 & 0 & 0 & 0 \\ 0 & 0 & 0 & 0 \end{bmatrix}. \tag{30}$$

This decomposition shows us how our ensemble-average derivation and isotropic-scattering assumptions result in two known Mueller matrices: The first is a combination of a linear attenuator and retarder matrix,[28] and the second is a depolarizer.[29]

4. Experimental Measurements

We have developed experimental procedures that allow us to measure the effects of the electric field in PLZT on such characteristics as scattering, depolarization, and the EO response. In these experiments we constructed a setup that produces a homogeneous electric field within our sample that is achieved by use of a parallel-plate capacitor configuration [see Fig. 1(a)]. By sandwiching our PLZT sample between two parallel gold-plated copper plates, which are much larger than the sample, we generate a constant electric field inside and outside the ceramic and avoid fringing-field inhomogeneities. The distance between plates d and the applied voltage V give us the electric-field strength $E = V/d$, and the thickness L of the PLZT is the optical interaction length.

In this experiment we use a He–Ne laser beam polarized at 45° relative to the direction of the applied electric field. The coherent light is transmitted through a spatial filter and recollimated to define the dc spatial frequency of the input optical field illuminating the entire PLZT sample (see Fig. 2). We use dichroic polarizers with an extinction ratio better than 1×10^{-3}. The transmitted light is captured by a lens and directed onto a Newport Si detector, Model 818-SL, and the total intensity is measured with a Newport Model 835 optical power meter.

Using the experimental setup outlined above, we measure the transmitted optical intensity versus an applied electric field (see Fig. 4) by using the five polarizer–analyzer orientations given in Eqs. (18)–(22). For comparison purposes we show twice the intensity values of the vertical and horizontal measurements, as we discuss below. We can see that

$$I_{0°,0°} \approx I_{90°,90°}, \qquad I_{0°,90°} \approx I_{90°,0°}. \tag{31}$$

Therefore in this case we may assume that these terms are equivalent and use the isotropic scattering approximation made in deriving the simplified Mueller matrix [Eq. (26)]. We can also see from the plot that all the intensity curves converge to the same value above 1.75×10^6 V/m. This convergence indicates that the light becomes completely unpolarized under the influence of a very strong electric field.

In Fig. 4 the maxima of the $I_{45°,45°}$ data are approximately equal to the $2I_{0°,0°}$ and the $2I_{90°,90°}$ data sets, which is consistent with our equations, since the maxima values, i.e., $\cos(\phi) = 1$, of Eq. (27) yield

$$I_{45°,45°_{\max}} = A(E) + U(E) = 2I_{0°,0°} = 2I_{90°,90°}. \tag{32}$$

Additionally, the minima are

$$I_{45°,45°_{\min}} = U(E) = 2I_{0°,90°} = 2I_{90°,0°}, \tag{33}$$

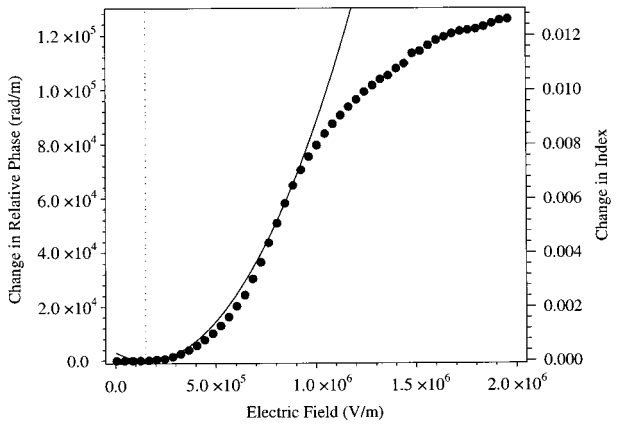

Fig. 5. Change in the relative phase calculated from measured data for PLZT 8.9/65/35 (circles). For comparison we also show the calculated change in phase obtained by use of a shifted ($E_0 = 1.5 \times 10^5$ V/m) electric field in the standard quadratic model (solid curve) with the quadratic EO coefficient $R = 17.0 \times 10^{-16}$ (m/V)^2. The change in the index of refraction is calculated by use of the linear relation $\Delta\phi/L = 2\pi\Delta n/\lambda$.

which again coincides with the measurements shown in Fig. 4. In Eqs. (32) and (33) we use a more complete notation showing the electric-field dependence of the coefficients.

Substituting Eqs. (28) and (29) into Eq. (27) we solve, using the simplified Mueller matrix, for the change in relative phase:

$$\phi = \cos^{-1}\left(\frac{I_{45°,45°} - I_{0°,0°} - I_{0°,90°}}{I_{0°,0°} - I_{0°,90°}}\right). \tag{34}$$

The calculated phase function is shown in Fig. 5. The smoothness of this curve represents the accuracy of our isotropic approximation. That is, intensity measurements with strong anisotropic scattering will result in a phase function with clear discontinuities. Therefore for some materials a fine resolution of the phase function could require including the variations of transmitted intensity owing to anisotropic scattering, i.e., making all seven of the required measurements [Eqs. (18)–(24)]. As we noted above [see Fig. 1(b)], up to 2×10^5 V/m electric-field strength the PLZT has relatively no EO response and the phase function remains flat. From 2×10^5 V/m to 1×10^6 V/m the EO phase response is roughly quadratic, and at higher electric-field strengths the response diminishes significantly, i.e., saturates, as discussed in Section 2.

Previous research has produced similar phase functions[1,10] that show the saturation of the EO effect at high field, with a maximum change in index of approximately 1×10^{-2}. However, the weak EO response of PLZT at low electric-field strength is often not present in published experimental data. We believe that this is due to the use of a surface-electrode configuration to characterize the materials' EO response.[10] In this configuration the electric field is not homogeneous, and it can be very difficult to calculate accurately the phase versus the electric-field function.

For simplification these PLZT compositions are usually assumed to have a quadratic EO response or a combination of a linear and a quadratic response. However, as can be seen from Fig. 5, the quadratic approximation does not account for the saturation at high electric fields, and neither model can account for the weak response at low field strength. We find that the use of a fifth-order polynomial achieves an excellent fit to the change in phase–index versus the electric-field data available. Although this material's EO response is dominated by the quadratic (Kerr) effect, the linear (Pockels) response might also be present. The higher-order terms in the fifth-order polynomial fit can be associated with material constraints that freeze the polarizability under weak fields and limit molecular deformation under high fields.

5. Conclusion

In this paper we have presented a new method for characterizing the polarization properties of scattering and depolarizing EO materials by using as an example PLZT 8.8–9.5/65/35 compositions. We showed that the optical field passing through bulk PLZT can be described by superposition of a nonscattered polarized component and a scattered depolarized component. Using the corresponding deterministic and stochastic Jones matrices, we have derived a simplified Mueller matrix representation in which only seven coefficients are required to describe the scattering and depolarizing EO device. Using Stokes vectors, we were then able to calculate the transmitted optical intensity for light passing through our device in terms of the seven corresponding coefficients.

By placing a PLZT device (that has a parallel-plate electrode geometry) between a pair of polarizers, we perform relatively simple (compared with Mueller matrix ellipsometry[30]) experimental measurements to solve for the unknown coefficients. As we vary the electric potential across the PLZT device, we generate a data set describing the coefficients of scattering, depolarization, and EO phase response as functions of the applied electric field. Experimental results show practically no EO response for PLZT under a weak electric field. This effect might not be observed with a traditional surface-electrode geometry, since the electric field can be very high near the electrode edges, even under small applied voltages. Our characterization shows distinctly different EO responses for weak, medium, and strong electric-field strengths. Therefore, for accurate simulation of changes in phase (or index of refraction) resulting from large electric-field gradients (e.g., surface-electrode devices), we must use a higher than second-order EO model.

Although PLZT has been shown to have anisotropic scattering, to reduce the number of unknowns in our Mueller matrix, we have assumed the simpler model of isotropic scattering. This can be justified on the

basis of the similarity between the measured intensities for the various polarized and depolarized components. Using the experimental data shown in Fig. 4, we have compared the intensities of the two orthogonal polarized components (A, B) and have found that the average difference is less than 2%, with a maximum of 5%. Comparing the intensities of the four depolarization-component intensities (U_1, U_2, U_3, U_4) gives an average difference of less than 4% (when dividing by the maximum depolarized intensity) and a maximum difference of 13%. Therefore within a less than 5% average error we can use the isotropic-scattering approximation to simplify our Mueller matrix to have only three unknown coefficients (A, U, and ϕ) and reduce the corresponding number of required experimental measurements.

The application of our characterization study, as discussed in this paper, to computer-aided design and device simulation is discussed in a second paper, also in this issue. We also continue to characterize bulk PLZT in terms of temperature and ac electric-field dependencies, as well as to characterize alternative EO materials.

Appendix A

1. Jones Matrix Formulation

For a uniform monochromatic TE plane wave incident on a nondepolarizing optical system, the outgoing plane wave can be described by

$$E_{x'} = J_{11}E_x + J_{12}E_y, \tag{A1}$$

$$E_{y'} = J_{21}E_x + J_{22}E_y, \tag{A2}$$

which can be combined in matrix form as

$$\begin{bmatrix} E_{x'} \\ E_{y'} \end{bmatrix} = \begin{bmatrix} J_{11} & J_{12} \\ J_{21} & J_{22} \end{bmatrix} \begin{bmatrix} E_x \\ E_y \end{bmatrix}, \tag{A3}$$

or by the simplified notation $\mathbf{E}' = \mathbf{JE}$, where the transformation by the optical element or system,

$$\mathbf{J} = \begin{bmatrix} J_{11} & J_{12} \\ J_{21} & J_{22} \end{bmatrix}, \tag{A4}$$

is called the Jones matrix.[20]

2. Kronecker Product

The Kronecker[23] (or direct product) for 2×2 matrices is given by

$$\mathbf{J} \otimes \mathbf{J}' = \begin{bmatrix} J_{11}J_{11}' & J_{11}J_{12}' & J_{12}J_{11}' & J_{12}J_{12}' \\ J_{11}J_{21}' & J_{11}J_{22}' & J_{12}J_{21}' & J_{12}J_{22}' \\ J_{21}J_{11}' & J_{21}J_{12}' & J_{22}J_{11}' & J_{22}J_{12}' \\ J_{21}J_{21}' & J_{21}J_{22}' & J_{22}J_{21}' & J_{22}J_{22}' \end{bmatrix}. \tag{A5}$$

3. Stokes to Coherency-Parameter Transformation

The coherency matrix, like the Stokes vector, can also be used to describe the polarization state of light and is defined by

$$\mathbf{C} = \begin{bmatrix} \langle E_x E_x^* \rangle & \langle E_x E_y^* \rangle \\ \langle E_y E_x^* \rangle & \langle E_y E_y^* \rangle \end{bmatrix}, \tag{A6}$$

where E_x and E_y are defined in Eq. (2). Although the standard notation for the coherency matrix is $\mathbf{J}$, we use the notation $\mathbf{C}$ to avoid confusion with our use of $\mathbf{J}$ for the Jones matrix. By use of Eq. (3) the relation between the Stokes and the coherency parameters can be written as

$$\begin{aligned} S_0 &= C_{xx} + C_{yy}, \\ S_1 &= C_{xx} - C_{yy}, \\ S_2 &= C_{xy} + C_{yx}, \\ S_3 &= j(C_{xy} - C_{yx}). \end{aligned} \tag{A7}$$

Presenting the coherency matrix as a 4×1 vector yields

$$\mathbf{C} = \begin{bmatrix} C_{xx} \\ C_{xy} \\ C_{yx} \\ C_{yy} \end{bmatrix}; \tag{A8}$$

then the transformation from the Stokes parameters to the coherency parameters can be given by the relation $\mathbf{S} = \mathbf{TC}$, where

$$\mathbf{T} = \begin{bmatrix} 1 & 0 & 0 & 1 \\ 1 & 0 & 0 & -1 \\ 0 & 1 & 1 & 0 \\ 0 & j & -j & 0 \end{bmatrix}. \tag{A9}$$

The authors thank James Thomas for his generous assistance. This study was funded in part from grants from the National Science Foundation, the Air Force Office for Scientific Research, and Rome Labs.

References

1. G. Haertling, "Electro-optic ceramics and devices," *Electronic Ceramics: Properties, Devices, and Applications*, L. Levinson, ed. (Marcel Dekker, New York, 1988), pp. 371–492.
2. J. Thomas and Y. Fainman, "Programmable diffractive optical elements using a multichannel lanthanum-modified lead zirconate titanate phase modulator," Opt. Lett. **20,** 1510–1512 (1995).
3. Q. W. Song, X. M. Wang, and R. Bussjager, "Lanthanum-modified lead zirconate titanate ceramic wafer-based electro-optic dynamic diverging lens," Opt. Lett. **21,** 242–244 (1996).
4. T. Utsunomiya, "Optical switch using PLZT ceramics," Ferroelectrics **109,** 235–240 (1990).
5. J. T. Cutchen, J. O. Harris, and G. R. Laguna, "PLZT electrooptic shutters: applications," Appl. Opt. **14,** 1866–1873 (1975).
6. P. Shames, P. C. Sun, and Y. Fainman, "Modeling and optimization of electro-optic phase modulator," in *Physics and Simulation of Optoelectronic Devices IV*, W. W. Chow and M. Osinski, eds., Proc. SPIE **2693,** 787–796 (1996).

7. C. E. Land, "Variable birefringence, light scattering, and surface-deformation effects in PLZT ceramics," Ferroelectrics **7,** 45–51 (1974).
8. E. E. Klotin'sh, Yu. Ya. Kotleris, and Ya. A. Seglin'sh, "Geometrical optics of an electrically controlled phase plate made of PLZT-10 ferroelectric ceramic," Avtometriya **6,** 68–72 (1984).
9. K. Tanaka, M. Yamaguchi, H. Seto, M. Murata, and K. Wakino, "Analyses of PLZT electrooptic shutter and shutter array," Jap. J. Appl. Phys. **24,** 177–182 (1985).
10. M. Title and S. H. Lee, "Modeling and characterization of embedded electrode performance in transverse electro-optic modulators," Appl. Opt. **29,** 85–98 (1990).
11. Y. Wu, T. C. Chen, and H. Y. Chen, "Model of electro-optic effects by Green's function and summary representation: applications to bulk and thin film PLZT displays and spatial light modulators," in *Proceedings of the Eighth IEEE International Symposium on Applications of Ferroelectrics*, M. Liu, A. Safari, A. Kingon, and G. Haertling, eds. (Institute of Electrical and Electronics Engineers, New York, 1992), pp. 600–603.
12. A. E. Kapenieks and M. Ozolinsh, "Distortion of phase modulation by PLZT ceramics electrically controlled retardation plates," Optik (Stuttgart) **63,** 333–339 (1983).
13. D. H. Goldstein, "PLZT modulator characterization," Opt. Eng. **34,** 1589–1592 (1995).
14. A. Yariv and P. Yeh, *Optical Waves in Crystals* (Wiley, New York, 1984), Chap. 5.
15. B. Mansoorian, "Design and characterization of flip-chip bonded Si/PLZT smart pixels," Ph.D. dissertation (University of California, San Diego, La Jolla, Calif., 1994), Chap. 2.
16. E. T. Keve, "Structure–property relationships in PLZT ceramic materials," Ferroelectrics **10,** 169–174 (1976).
17. G. H. Haertling and C. E. Land, "Hot-pressed (Pb,La)(Zr,Ti)O_3 ferroelectric ceramics for electrooptic applications," J. Am. Ceram. Soc. **54,** 1–10 (1971).
18. M. Ivey, "Birefringent light scattering in PLZT ceramics," IEEE Trans. Ultrason. Ferroelec. Frequen. Contr. **38,** 579–584 (1991).
19. R. A. Chipman, "The mechanics of polarization ray tracing," in *Polarization Analysis and Measurement*, D. H. Goldstein and R. A. Chipman, eds., Proc. SPIE **1746,** 62–75 (1992).
20. M. Born and E. Wolf, *Principles of Optics*, 6th ed. (Pergamon, New York, 1989), pp. 554–555.
21. R. M. A. Azzam and N. M. Bashara, *Ellipsometry and Polarized Light* (North-Holland, Amsterdam, 1987), Chap. 2.
22. A. E. Kapenieks, "Mueller matrix determination for the transparent ferroelectric PLZT ceramics in the transverse electric field," Lat. PSR Zinat. Akad. Vestis Fiz. Teh. Zinat. Ser. **6,** 61–65 (1980).
23. F. W. Byron and R. W. Fuller, *Mathematics of Classical and Quantum Physics* (Dover, New York, 1970), Chap. 3.
24. K. Kim, L. Mandel, and E. Wolf, "Relationship between Jones and Mueller matrices for random media," J. Opt. Soc. Am. A **4,** 433–437 (1987).
25. R. M. A. Azzam, "Propagation of partially polarized light through anisotropic media with or without depolarization: a differential 4×4 matrix calculus," J. Opt. Soc. Am. **68,** 1756–1767 (1978).
26. J. Goodman, *Statistical Optics* (Wiley, New York, 1985), Chap. 8.
27. S. M. F. Nee, "The effects of incoherent scattering on ellipsometry," in *Polarization Analysis and Measurement*, D. H. Goldstein and R. A. Chipman, eds., Proc. SPIE **1746,** 119–127 (1992).
28. R. A. Chipman, "Polarimetry," in *Handbook in Optics*, M. Bass, ed. (McGraw-Hill, New York, 1995), Vol. 2, Chap. 22.
29. C. Brosseau, "Mueller matrix analysis of light depolarization by a linear optical medium," Opt. Commun. **131,** 229–235 (1996).
30. R. M. A. Azzam, "Ellipsometry," in *Handbook in Optics*, M. Bass, ed. (McGraw-Hill, New York, 1995), Vol. 2, Chap. 27.